Chapter 7: Identifying Wetland Zonation and Inundation Extent by Using Satellite Remote Sensing and Ground-Based Measurements

by
Elijah W. Ramsey III[a], Stephen C. Laine[a], Gene A. Nelson[b], Sijan K. Sapkota[b], Marshall L. Strong[a], Jennifer K. Wooderson[b], Richard H. Day[a], Ruth E. Spell[a], Dal K. Chappell[a], Troy L. Stoute[b], Robert G. Kirkman[b], and Mark A. Books[b]

[a]*U.S. Geological Survey*
National Wetlands Research Center
700 Cajundome Blvd.
Lafayette, Louisiana 70506

[b]*Johnson Controls World Services Inc.*
NWRC Operations
700 Cajundome Blvd.
Lafayette, Louisiana 70506

Abstract: We developed a number of satellite remote sensing tools that could dynamically monitor coastal resource change and response to sea-level rise caused by global climate change and other natural (e.g., fire, storm impact, herbivory) and human (e.g., fire, flood control structures, oil spills, mitigation, and restoration) impacts. Together, these tools could immediately help provide improved coastal regulation and management and eventually produce improved long-term simulations given a variety of "what if" scenarios. Within the package of tools, new methods were developed to dynamically detect flooding under grass canopies, generate coastal maps with microtopography within about 8 to 14 cm, detect and predict the time-since-burn of a black needlerush (*Juncus roemerianus*) marsh up to 900 days after the burn, and combine sensors of different spatial and spectral ranges and resolutions to provide a higher spatial resolution and a more refined coastal classification and detection system.

Introduction

Coastal resources already threatened by natural and human-induced stress are faced with further degradation unless action is taken to provide for increases in sea level and continued development. As part of an effort to provide timely and accurate information on a regional-to-international scale, we developed a number of satellite remote sensing tools that could dynamically monitor coastal hydrology and wetland changes. Equipped with these tools, researchers and managers can begin to link coastal hydrology to vegetation characteristics and, consequently, develop a better understanding of the expected responses of the coastal ecosystem to sea-level rise. Furthermore, these tools provide methods for monitoring, and eventually predicting, coastal response to continued development and natural (e.g., fire, herbivory, storm impact) and managed (e.g., fire, flood control structures, coastal mitigation, and restoration) forces. In turn, these methods could provide information that resource managers and regulatory agencies need to develop improved and consistent wetland response models and provide a basis for allocating financial resources and directing responses to influences causing wetland change or loss.

Background

The formation and health of wetland ecosystems is directly linked to surface hydrology (Imhoff and Gesch 1990). In coastal wetlands, hydrology is dominated by surface topography, terrestrial surface drainage, soil hydraulic character, and local tidal dynamics. The topographic contour and water level, however, determine the frequency, duration, and depth of flooding. As a consequence, critical controls of wetland type, productivity, and health, such as the level of soil salinity, the saturation of the soil, and the balance between particle import and export, are ultimately tied to the topography (Chabreck 1970; Redfield 1972; Stumpf 1983; Stevenson et al. 1985; Hine et al. 1988; Reed 1989; Imhoff and Gesch 1990; DeLaune et al. 1994; Leonard et al. 1995). Forecasting how changes in these controls (e.g., involving new wetland creation, wetland restoration, sea-level rise) will affect present and future wetland species zonation requires identifying the relationships between hydrology and wetland type and health.

Currently, the ability to associate hydrology with wetland type and health is limited because of the lack of both high detail in topographic surface maps (McKee and Patrick 1988) and timeliness in the production of new coastal wetland maps. Available U.S. Geological Survey (USGS) topographic maps for the Gulf of Mexico coast, for example, use a 150-cm contour interval, while the average shore-normal elevation gradient can be as low as 12 cm per kilometer for tens of kilometers (Fruh et al. 1973). Even within this shallow gradient, wetlands are diverse systems that exhibit extreme variations in areal extent, temporal duration, and spatial complexity (e.g., Chabreck 1970). In addition, wetland vulnerability and intensity of use can further complicate the spatial and temporal patterns. For example, storms, herbivory, and fire can not only confuse the classification of wetland type and indicators of health, but they can also affect the response of a wetland to sea-level rise. Monitoring tools are needed that can discriminate wetland types and health and also identify where wetland change has occurred, what the nature of the change was (from-to), and what the sequence of change was (e.g., recovery). Maps produced by the National Wetlands Inventory provide some of this information (Peters 1994), but the enormous investment in photography acquisitions and interpretation results in a turnaround of nearly 10 years for new map production (Wilen and Frayer 1990). To be effective, the information derived from the remote sensing data must not only be highly detailed, but also timely and cost effective (Teuber 1990). Satellite and aircraft remote sensing can provide timely and cost effective data, but techniques must be developed that can transform the data into information about wetland responses to changes in the hydrologic regime as a function of global climate change and sea-level rise scenarios.

Today, many satellites carry a variety of remote sensing instruments. Of these, optical sensors have the longest history of being used for mapping wetland types and monitoring wetland changes (e.g., Weismiller et al. 1977; Klemas et al. 1980; Hardisky et al. 1986; Jensen et al. 1987; Ramsey et al. 1992, 1993). These sensors include the Landsat Thematic Mapper (TM) and, more recently, SPOT high resolution visible sensors onboard satellite platforms. Traditionally, optical sensors provided nearly all the images of wetland areas; however, with the launch of Seasat in 1978, radar has slowly gained importance in wetland mapping (Lyon and McCarthy 1981; Ramsey 1998).

Satellite optical imagery offers synoptic coverage but is constrained by the restricted ability of visible and near infrared light to penetrate vegetative canopies (Ormsby et al. 1985). Furthermore, optical systems are limited to favorable weather and daylight, hampering the ability to respond effectively to rapidly changing wetland conditions. Radar imaging systems can overcome many of these limitations by providing better canopy penetration and the capability for day and night acquisitions nearly independent of weather conditions (Ormsby et al. 1985; Dobson et al. 1992; Ramsey et al. 1994; Ramsey 1998).

Integration of remotely sensed optical and radar information could provide much of the information necessary for linking hydrology and wetland type and health. In developing tools to link wetland type and health to hydrology, our research combined aircraft and satellite optical and radar data. Together these sensors provided the first step in building an integrated remote sensing system for dynamic monitoring of wetland hydrology and change and,

ultimately, for predicting coastal vegetation responses to changes in sea-level and storm occurrence frequency and intensity. Our objectives were to establish methods that use optical and radar sensors to detect flooding, improve the coastal marsh topographic information currently available, provide timely, high definition (as many wetland types as possible), high spatial detail (to about 10-m resolution) wetland maps, dynamically detect and monitor the impact and recovery of wetlands affected by hurricanes, herbivory, saltwater intrusion, and management practices (e.g., fire), and finally, to link the hydrologic regime to the current distribution of coastal vegetation. The study area is the St. Marks National Wildlife Refuge (NWR) in the Big Bend area of Florida (Fig. 7-1). The primary focus of the study at the beginning was a black needlerush (*Juncus roemerianus*) coastal marsh; however, increasingly work has extended into the transitional vegetation (e.g., palmetto, fresh marsh) and more inland pine and bottomland forests.

Remote Sensing of Wetland Type and Hydrology

Detecting Coastal Flooding

Satellite radar was used to map tidal flooding (Ramsey 1995). Six synthetic aperture radar (SAR) images of the St. Marks NWR were acquired from ERS-1 satellite orbits between May and November 1993. The radar images were collected during flood and nonflood events (Fig. 7-2). To perform the multidate analysis of the SAR images, it was necessary to first convert the relative radar returns to comparable units and the relative image coordinates to a common georeferenced base map. Near-continuous recordings of ground-based hydrology measurements, taken during the time of the SAR image collections, were then used to link marsh flooding to lowered radar returns. Flood-extent contours extracted from the radar images (PCI Geomatics 1998) and calibrated with point-water depth measurements showed marsh elevation could be estimated to about 8–14 cm, compared to the 150-cm topographic contours previously available. This close estimate demonstrates that ERS-1 SAR can be used to discern flooded from nonflooded black needlerush marsh. Even though restricted to a particular marsh type and to a single SAR sensor, this ability provides a tool for discerning the occurrence and monitoring the extent (within about 25–50 m) of flooding regionally, day and night, and during almost any type of weather. Additionally, when used with ground-based point measures of water level, this tool can be used to generate microtopography.

Generating Coastal Microtopography

A topographic surface map of the low-lying coastal marsh was created by using three flood extent vectors digitized from ERS-1 SAR images and two elevation contours from USGS topographic quadrangles (Ramsey 1995; Ramsey et al. 1998a). Point measurement of water depth at the times of the SAR collections allowed conversion of

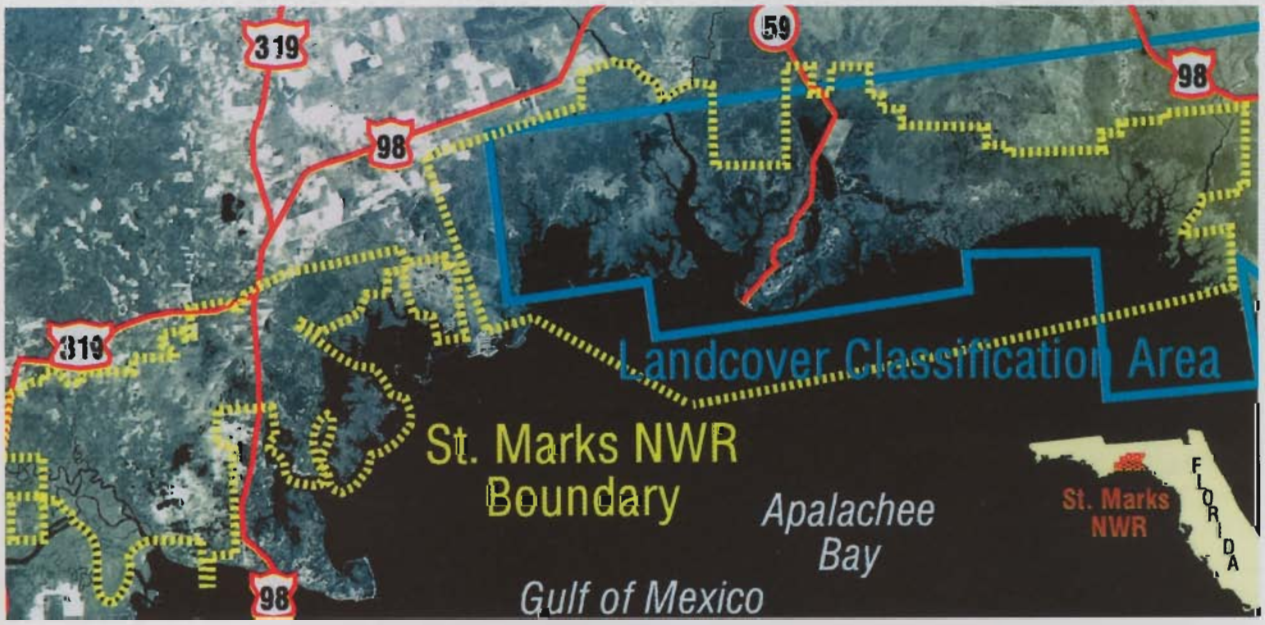

Figure 7-1. Landsat Thematic Mapper band 5 (mid-infrared) image of the study site at the St. Marks National Wildlife Refuge (NWR) in the Big Bend area of Florida. This image was collected on August 25, 1993 and was acquired from USGS EROS Data Center. The blue outline encompasses the actual study area.

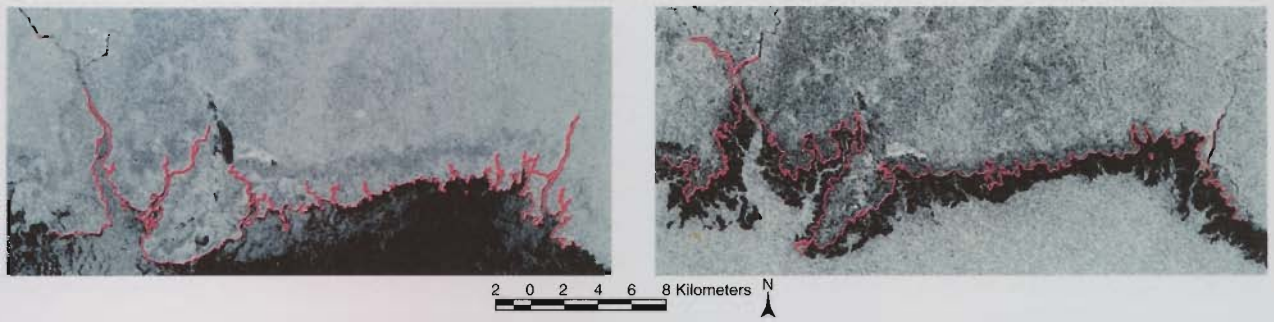

Figure 7-2. ERS-1 SAR images collected on October 18 (left; nonflooded) and September 13 (right; flooded) of 1993 of a black needlerush marsh within the St. Marks NWR. Flooding lowered the radar return in the coastal marsh areas resulting in a darker image. (Ramsey 1995, with permission of Taylor & Francis).

the flood extent vectors to topographic contours related to mean sea level (within about 8–14 cm accuracy). Generation of the topographic surface map was accomplished with a surface gridding algorithm (Smith and Wessel 1990; Wessel and Smith 1991; Fig. 7-3).

Verification of the resulting topographic map was performed by comparing the map to field-measured elevations taken at 10-m intervals along five shore-normal transects (Fig. 7-3). Field measurements were transformed into elevations by linking to USGS primary benchmarks.

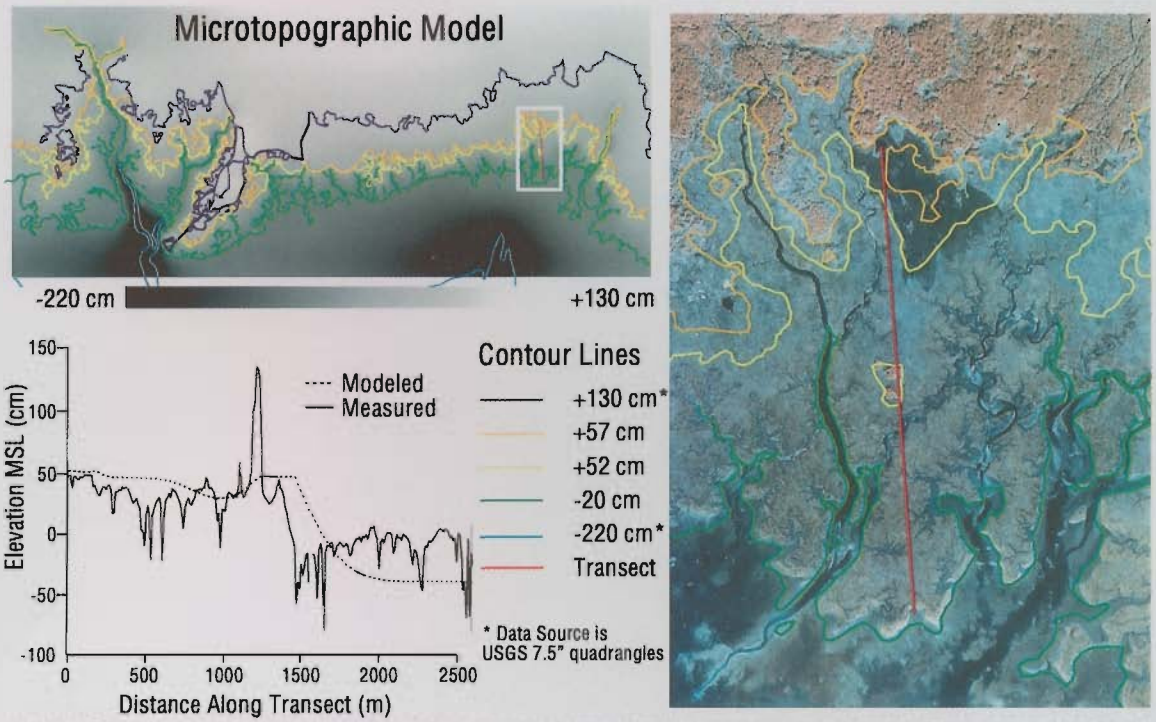

Figure 7-3. The modeled topographic surface map with one transect location. Relief recordings were collected at 10-m intervals and transects were linked to established USGS benchmarks to evaluate the actual mean sea level. Three of the five topographic contours were developed with ERS-1 radar data and on-screen image processing to detail beyond available traditional topographic contours data; two topographic contours (+130 cm and -220 cm) were taken from USGS standard 1:24,000 quadrangles. The resultant topographic surface has < ± 15 cm absolute mean error for the entire area (figure modified after Ramsey et al. 1998a, with permission of Coastal Education & Research Foundation, Inc.). Before this study, the available topographic resolution for this area was about ± 150 cm.

Errors in marsh topography resulting from the surface gridding algorithm were mainly associated with the lack of contours in areas such as narrow-to-broad plateaus and topographic highs and lows and the misplacement of flood extent vectors in sparsely vegetated high marsh, at convoluted marsh-forest boundaries, and at topographic depressions. Overall, the standard deviation of differences between measured and predicted elevations at 747 points was 19 cm. Excluding abrupt boundaries and topographic highs and lows outside the range of available contours, the standard deviation of the differences averaged about 14 cm (568 observations), with most observations around 8 cm. These results suggested a 5- to 9-factor improvement over the 150-cm topographic resolution previously available for this area. With this topographic mapping tool, more realistic simulations of flood extent, duration, and depth can be generated at unprecedented spatial and topographic resolutions. What is now required is a landcover classification that can take advantage of this improved spatial and topographic detail.

Classifying Coastal Resources

Georegistered color infrared (CIR) photography, Landsat TM, and ERS-1 SAR images were combined to create a map of the marsh and upland vegetation of the refuge (Ramsey et al. 1998b). Classifications using only CIR or only TM produced mixed results, with confusion apparent between marsh and forest classes. Furthermore, spatial definition in the TM classification was inadequate, especially in defining features such as hummocks, transition zones, small channels, and heterogeneous and mixed interior forest areas. To alleviate these problems, CIR (for better spatial detail), TM (for higher spectral clarity; six reflective bands), and SAR (for greater textural information) were combined into one data base.

The CIR, originally scanned and mosaicked to a 3-m spatial resolution, was resampled to a 10-m spatial resolution. The TM and SAR images were resampled from 25-m to 10-m spatial resolution. The TM, CIR photographic, and SAR image data were classified by using a clustering algorithm (PCI Geomatics 1998), a computational procedure that combines groups of related variables. Instead of classifying each image separately (Schriever and Congalton 1993; Wotler et al. 1995), the six TM reflective bands, the green CIR band, and a single SAR C band (VV, vertical send and return) were merged into a single classification analysis (Fig. 7-4 a-c). To further improve separation between classes, a progressive classification scheme was used (Jensen et al. 1987; Ramsey and Laine 1997). The 14 final classes included water, marsh, and forest classes, as well as burned marsh and burned forest (Fig. 7-5).

A class-stratified, random-sampling technique (Congalton 1988) was used to generate classification error estimates for the study area. The same CIR photography used in the classification was used as reference data. Fifty samples were used for each class (Congalton 1991).

Even though the overall accuracy was 73%, class definition and spatial detail were greatly improved compared to classifications using solely TM or photography. Multiple marsh and forest types were identified with only minor to moderate overlap in some classes, and small-scale features (down to around 10 m) were detected. Even with the use of progressive classification and multiple image types, however, some confusion still existed between classes. In these cases, final class determination was based on retaining the landscape pattern while minimizing the classification error. This procedure was especially necessary in transition classes (e.g., low-to-medium marsh, high-to-fresh marsh, fresh marsh to fringe forest). Even though higher classification accuracy could have been obtained by aggregating these transitional classes, the classification more correctly represented the actual landcover pattern in this extremely convoluted, nearly monotypic landscape. This new classification tool improves the mapping capabilities of the widely used TM images spatially and in the amount of detail, thus providing the ability to discern subtle differences in the vegetation canopy even within the same species.

Monitoring Damage and Recovery

As an example of monitoring impacted wetlands, the recovery of burned black needlerush marsh areas using radar sensors was examined (Ramsey et al. 1998c). The extent of burned marsh areas identified on a December 1992 CIR photography mosaic were delineated with onscreen digitizing (PCI Geomatics 1998). These polygons were then overlaid on July 1993 ERS-1 (C band VV polarization, defined previously), April 1992 USGS Star-1 (X band HH polarization, horizontal send and return), and July 1993 P3 Orion (L band VV, VH [vertical send and horizontal return], and HH polarizations) radar images (Fig. 7-6 a-b). Mean and standard deviation of the data values within each polygon were extracted from each image. These univariate statistics were entered into a common data base along with the approximate times of each burn. Burn times were from a burn log recorded at the refuge and from direct observations. Plots of the radar means for each burn site versus the time-since-burn and associated regression statistics were generated (SAS 1989).

Inspection of the plots and the regression statistics showed that significant relationships ($p < 0.05$) existed between burn recovery and the ERS-1 C band VV polarization and P3 Orion L band VH polarization (Fig. 7-7 a-b). No significant relationships existed between single L band VV and HH returns and the time-since-burn. Even though the USGS radar returns were not correlated to the time-since-burn, the data suggested burns could be identified

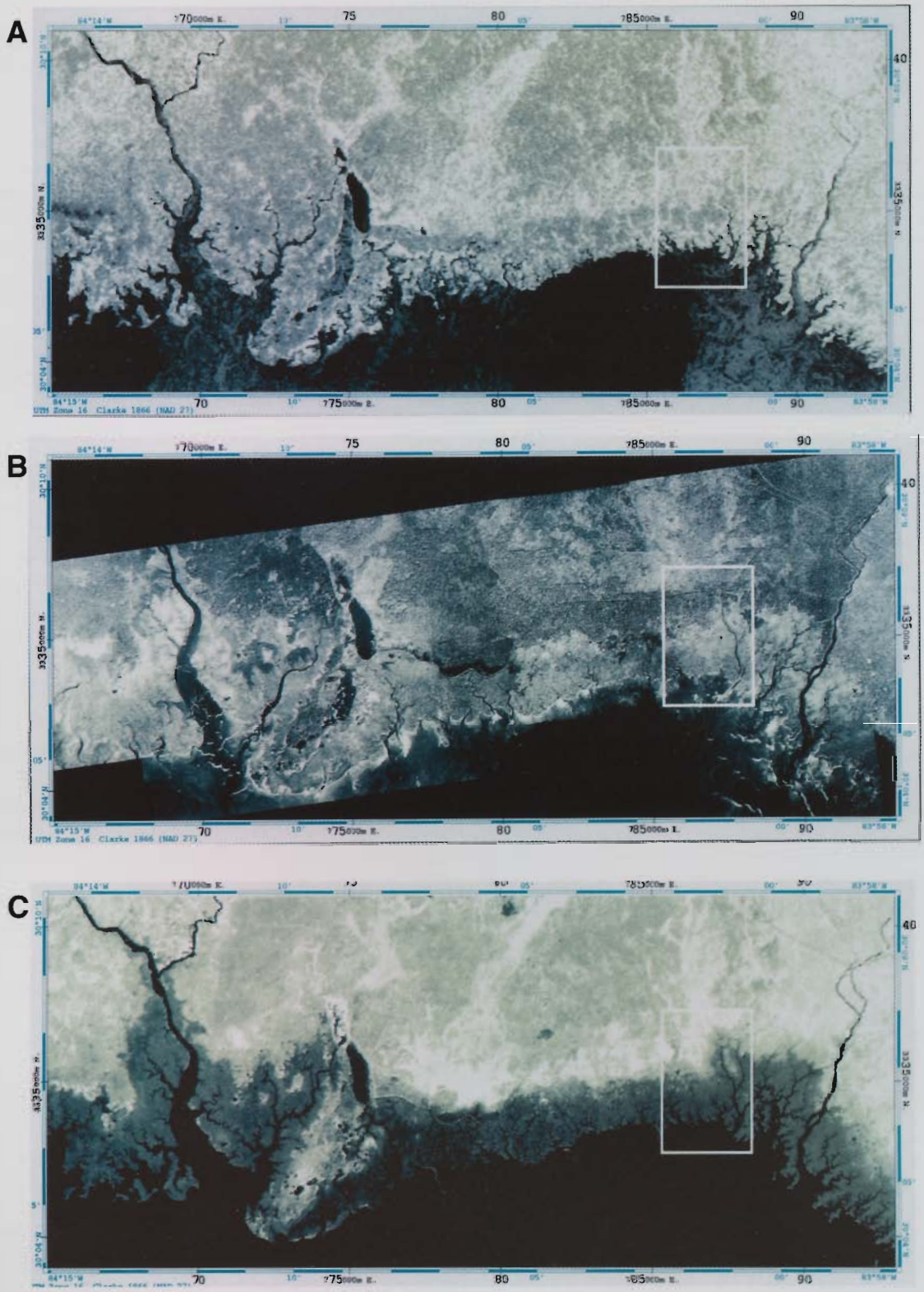

Figure 7-4. Comparison of different data sources. Spatial detail as well as vegetation classification were highly improved by combining the three data sources: (A) green band (0.5-0.6 µm) CIR photography; (B) ERS-1 SAR C band VV polarization; and (C) Landsat Thematic Mapper (TM) band 4 (0.8-0.9 µm). The CIR photography was resampled from original 3-m resolution to a 10-m resolution and ERS-1 SAR and TM from approximately 25-m to a 10-m resolution.

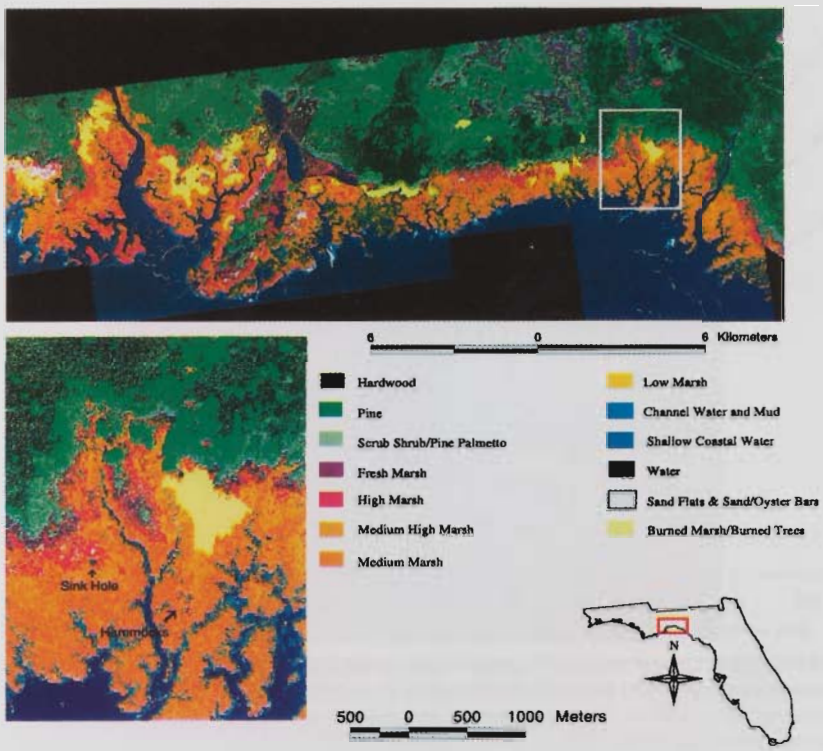

Figure 7-5. Classified map generated from a combination of the three data sources (see Fig. 7-4): high resolution CIR photography, Landsat Thematic Mapper imagery, and ERS-1 SAR imagery shown at a final 10-m spatial resolution. For visual clarity sand flats and oyster bars/sand bars are combined (modified after Ramsey et al. 1998b, with permission of Kluwer Academic Publishers).

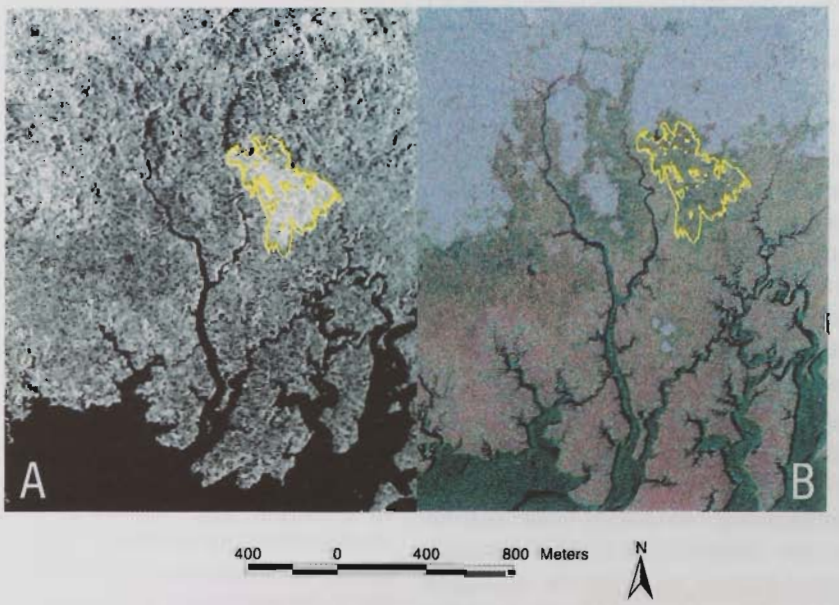

Figure 7-6. Monitoring the recovery of a burned marsh. The burned polygons extracted from color infrared (CIR) photography were overlaid on the radar imageries. (A) The April 1992 USGS Star-1 SAR X band HH polarization and (B) the July 1993 P3-Orion L band multiple polarizations (e.g., HH [red], VV [green], and VH [blue]). The USGS Star-1 and P3-Orion SAR images were collected from aircraft. The outlined area shows a marsh burn that occurred in March 1991.

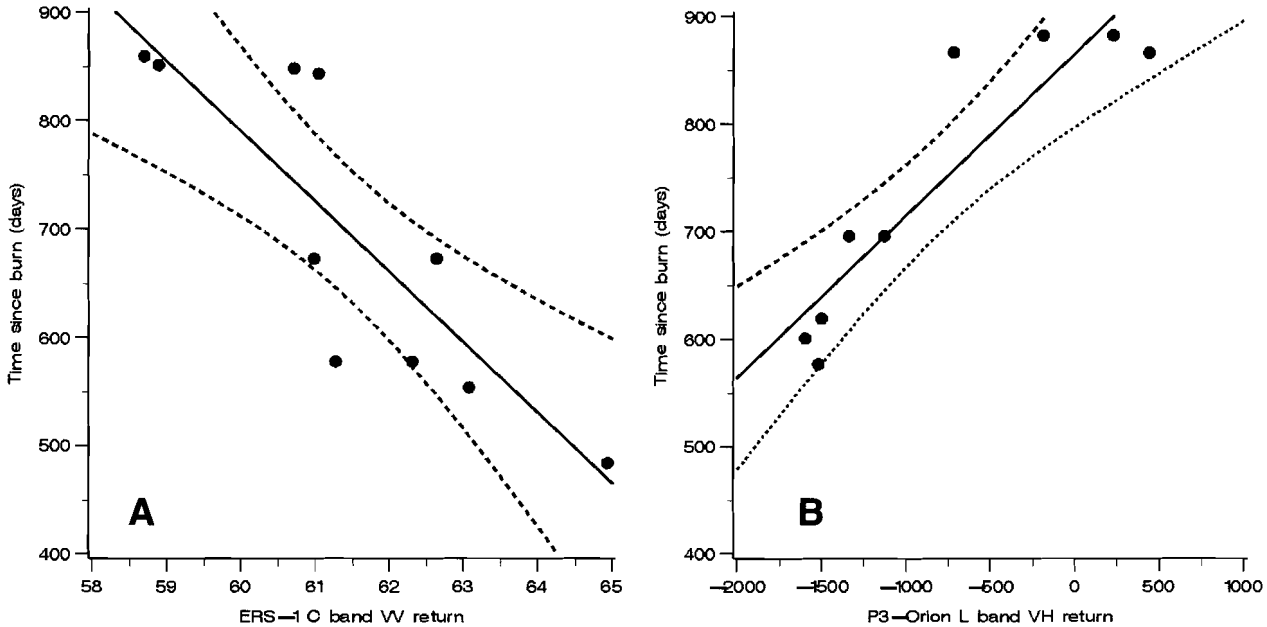

Figure 7-7. Scatter plots of number of days since burn versus signal return from different burned-marsh study sites. Solid lines indicate the predicted linear regression equation, and dashed lines indicate a 95 percent confidence interval of the predicted equation. (A) ERS-1 C band VV polarization and (B) signature difference between the burned and control sites of the P3 Orion L band VH polarization. Both SAR images were collected in July 1993.

with this radar at incident angles (scan angle of sensor) between 70° and 77°.

Overall, the combined data suggested that available ERS-1 satellite and P3 Orion aircraft radars could estimate time-since-burn of between 400 and 900 days for the black needlerush marsh. From the time of burn up to about 400 days, USGS Star-1 radar could detect a burnt marsh at incident angles less than 77°. Expanded to a regional level, these tools would not only aid in correctly detecting change and monitoring recovery, but could help in understanding how wetlands respond to burning and other acute stresses such as oil spills, herbivory, and storm impacts. This knowledge in turn could aid in understanding how these impacts may affect the wetland's ability to respond to rising sea levels and storm impacts.

Linking Hydrology to Coastal Resources

In the previous sections, we demonstrated our ability to detect and monitor coastal hydrology and vegetation type and status. A final objective of our study is to develop dynamic models to explain changes in the coastal landscape. Reaching this objective requires us to link the vegetation characteristics to the hydrologic regime. Establishing this link allows us not only to better understand what affects vegetation health but also to forecast future distributions of coastal resources given different scenarios of sea-level rise, storm occurrence frequency and intensity, and human development. To this end, we have developed and preliminarily tested a flushing model to explain the changes in coastal landscape by linking the hydrologic regime (e.g., inundation extent—duration and depth, soil moisture, flushing, salinity) to the current and predicted distribution of coastal resources (e.g., vegetation type, dead and live biomass, structure [density, orientation, height, leaf property, and woody material]).

The flushing model is based on predicted and measured water level and salinity and modeled microtopographic data. The model continuously flushes the coastal area, generating duration and depth of flood events over time (Fig. 7-8). Initial results indicated tidal flushing and the depth of inundation can explain up to 69% of the variation in the coastal resources (Ramsey, unpublished data). This model is being validated with site specific measurements. These are simplistic predictions that do not account for factors inhibiting or exacerbating coastal resource loss (e.g., erosion, shoreline protection structures, vegetation loss), but with refinement will at least give resource managers and coastal planners a reasonable long- and short-term look at possible consequences of sea-level rise, unusual flooding due to excessive rain, saltwater intrusion, storm impacts, and human developments.

Summary

Remote sensing tools were developed based on aircraft and satellite optical and radar data to map flooding, generate microtopography, refine landcover classification, and

Platform Sites	Observed 0-5 ppt	Modeled 0-5 ppt	Observed >10 ppt	Modeled >10 ppt	Observed %Flooded	Modeled %Flooded	Pooled %Flooded
Saline Low Marsh	65.61	42.58	11.03	18.55	48.2	40.5	7.5
Saline High Marsh	78.68	47.04	0.95	17.33	44.8	25.7	35.4
Saline High Marsh	72.86	49.40	0.00	17.03	42.0	22.5	12.6
Fresh Marsh	56.09	43.48	4.38	18.46	49.1	32.9	49.5
Saline Marsh	56.21	43.16	1.24	18.42	53.2	34.6	27.0
Fresh Marsh	64.74	49.40	14.69	17.03	41.5	22.5	43.4
Upland Forest	Not flooded during time of measurements.						

Replicate Sites Transition Sites Transition Sites

Figure 7-8. Comparison of actual water level and salinity data with the data obtained as an output of the flushing model. Five hydrology sites of eastern St. Marks NWR, Florida, are shown on the photographic subset. The data from three channel sites are placed at the freshwater input and where the river drainage channel bifurcates (saline input and freshwater export - shown downstream of the actual location for clarity). The observed percentages were tabulated from the data collected on site between Jan. 18 and Dec. 16 of 1997 whereas the modeled percentages are the output of the flushing model over the same time period with modeled microtopographic data and actual water level data (from one channel site) as inputs. The summary is preliminary and includes unequal observations due to equipment failures. An average of 7,000 observations were used in comparing modeled and observed salinity and flooding. Some of the differences in observed and modeled salinity may be due to the long periods of pooled water at the sites and the exclusion of freshwater inputs in the model (Ramsey, unpublished data).

detect and monitor change in a coastal wetland. These tools, and tools in development, will be used to link vegetation type and health to surface hydrology and, ultimately, to simulate the vegetation response to sea-level rise and increasing occurrence of storms that may result from global climate change. Additionally, tools are actively being developed to measure and monitor soil moisture and vegetation biomass as necessary additions to complete the link between hydrology and vegetation type and health. In combination, the tools are the beginning of an integrated remote sensing system for dynamic monitoring of hydrology and landcover change day and night, during any weather conditions, and at a higher spatial resolution and landcover detail with less manpower than is now possible with conventional techniques and tools.

Acknowledgments

We thank James Burnett, Joe White, John Fort, and Doug Scott of the U.S. Fish and Wildlife Service for allowing access to St. Marks National Wildlife Refuge, Florida, and helping us in field data collection. We also thank Kevin McRae, Allison Smith, Katy Golden, and

Elizabeth Wilson for their long hours of field work, data tabulations, and preliminary analyses. Dr. Ross Lunetta of the U.S. Environmental Protection Agency and NASA personnel Tom Chrien and Dr. Robert Green provided color infrared photography and Thematic Mapper Simulator and airborne visible/infrared imaging spectrometer (AVIRIS) data. Dr. Jim Verdi of U.S. Navy, Naval Air Warfare Center, furnished us with the P3-Orion SAR imagery. An original, classified map of the study site was provided by the Florida Game and Fresh Water Fish Commission. We also thank Dirk Werle of AERDE, Inc. (Canada), Ed Jurkevics of PCI Geomatics, and personnel of Radarsat, Inc. (Canada) for technical support and training. G.A. Borstad Associates, Ltd. of Canada provided hyperspectral image data. We appreciate the work of Beth Vairin of U.S. Geological Survey and Daryl McGrath of Johnson Controls World Services for editing this manuscript.